Use of Abaqus Explicit for Composite Sandwich Damage Prediction during Bird Impact

M. Al-Khalil, E. Kirtil, R. Rigby

Airbus

***Abstract**: A method development program of testing and simulations was carried out to develop bird impact NLFEA capabilities of composite sandwich damage prediction and bird dispersion after penetration of the primary layer using Abaqus Explicit. Curved composite honeycomb panels (referred to as J-Nose) representing typical composite wing Fixed Leading Edge (FLE) structure were subjected to bird strike to generate data for method validation. The test campaign was tailored to produce various levels of damage and modes of failure; from minor localized core/skin damage to panel perforation. In all tests high speed video were installed to capture the behavior of the structure during the impact. In some tests, fully instrumented witness panel was installed to enable measurement of deformation as a measure of bird residual energy and dispersion after bird penetration of the sandwich panel. FE models were created of the tested structure and analyzed using ABAQUS Explicit and the results were compared with tests. The analysis performed used a standard Lagrangian bird model developed and validated at Airbus over many years. In general, good correlation was obtained between tests and simulations results. It is known that Lagrangian bird models suffer from numerical instability in case of impacting sharp edges due to element distortion. To avoid such numerical difficulties, the SPH capability available in Abaqus/Explicit was used to generate a representative SPH bird model. Test cases were re-analyzed with the SPH bird model and results compared to the Lagrangian approach. A summary of bird impact simulations and correlation against tests is presented in this paper.*

Keywords: Aircraft, Wing, Leading, Edge, Bird, Damage, Impact, Composites, Sandwich

1. Introduction

Bird impact incidents on aircraft are not uncommon and they can cause structural and system damage. Although measures have been implemented to prevent bird impacts from occurring, it is impossible to prevent them totally. Further details regarding statistical reports related to bird impact incidents can be found in [1-3]. All forward facing components of an aircraft are most susceptible to bird strike such as leading edges of the wings and empennage, engine fan blades and inlet, windshield, window frame, radome, landing gear and forward fuselage as illustrated in Figure 1. The aviation authorities require that all aircraft structures in the vulnerable zones must be designed to assure capability of continued safe flight and landing of the aircraft after bird impact (EASA CS 25.631).

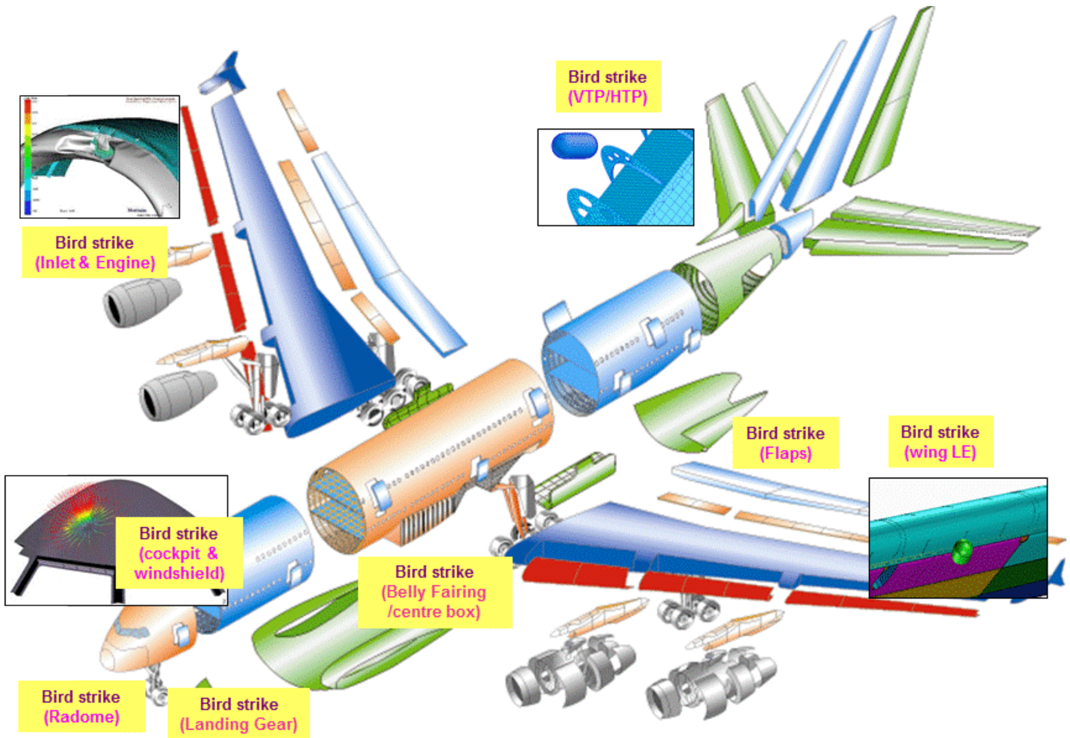

Figure 1 Illustration of aircraft components exposed to the risk of bird impact

Bird impact on aircraft structure is a complex phenomenon because of the high number of variables involved. Such variables include material characteristics of the impacted structure and bird behaviour and its interaction with the aircraft structure i.e. accurately predicting the level of pressure/forces transmitted to the structure. Traditionally, aerospace manufacturers rely heavily on tests, supported by empirical equations, for design and certification of aircraft subjected to bird impact. Such methods are not only time-consuming and expensive but they could lead to conservative design, resulting in weight penalty. In addition, such tests are subject to a degree of uncertainty due to the lack of consistency in bird impact test results for the same bird strike test configuration.

With the increase of finite element software tools capabilities and hardware computing power, it is now becoming more realistic to use such tools to develop finite element methods for predicting the behaviour of aircraft structures subjected to bird impact. However, it is important to emphasize that the analysis/numerical techniques must be validated through correlation with tests on sufficiently representative structure.

For almost two decades, Airbus has been involved in the development of bird strike methodologies for aircraft structures, (mainly for metallic but more recently for composite) and works closely with other Aerospace partners. A typical example of bird strike simulation and correlation with test on generic fixed leading structure, shown in Figure 2, was performed in collaboration with SONACA Aerospace manufacturer.

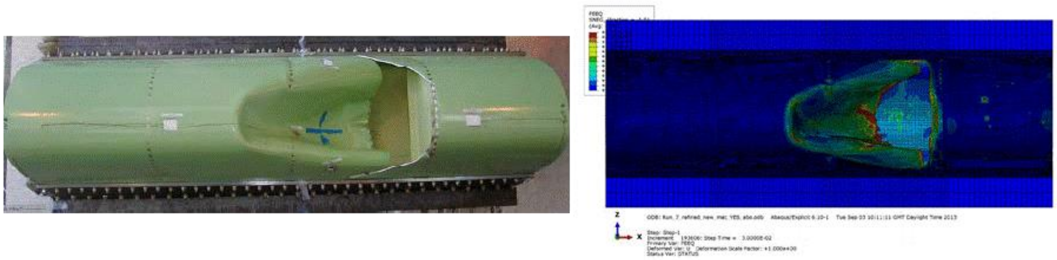

Figure 2 Simulation (ABAQUS Explicit) and test of bird impact on generic fixed leading edge structure

Composite materials including sandwich construction are increasingly being used for aircraft structures driven by high stiffness and strength to weight ratios. One of the main challenges of using composite structure is their susceptibility to impact damage. Therefore, understanding their behavior and in particular failure mechanisms is critical if the full benefit of using composites is to be exploited.

Bird impact nonlinear finite element methodology development and validation for composite sandwich J-Nose structure (situated in the wing leading structure) was performed using ABAQUS Explicit. Tests were performed to generate data for correlation with simulations. The analysis performed used a standard Lagrangian bird model developed and validated at Airbus. As part of ongoing bird modelling enhancement, Smooth Particle Hydrodynamics (SPH) capability within ABAQUS Explicit V613.3 was used and correlated with tests and Lagrangian approach. This paper outline a summary of the work performed including bird impact simulations and correlation with test results.

2. Method Validation

A bird strike test campaign was performed on a number of composite honeycomb panels, representative of a typical composite Fixed Leading Edge structure referred to a J-Nose. The aim of the test campaign was to provide test data for correlation with ABAQUS Explicit for method validation in particular for a) material failure prediction and b) predictive capability for secondary impact and dispersion after bird penetration of the J-Nose. It is important to note the impact scenarios considered such as impact angle, bird impact velocities and impact locations do not represent any specific aircraft flight configuration. The test campaign was tailored to produce various levels of damage and modes of failure; from minor localised core/skin damage to panel perforation. In all tests, high speed video cameras were installed at various positions to capture the behaviour of the structure and bird dispersion during the impact. Bird mass of 4 lb (1.81 kg) was used for all the test campaign and this is in-line with the certification requirement of wing leading edge structure. In some tests, a fully instrumented witness panel was installed to enable measurement of deformation as a measure of bird residual energy and dispersion after bird penetration of the J-Nose. Finite element models were created of the tested structure and analysed using a standard Lagrangian bird. However, SPH bird was also used for the test cases related to secondary impact and the simulation results are presented in Section 3. It is not possible to present all the results and therefore a sample of simulations and correlation with tests will be briefly outlined in this paper.

ABAQUS /CAE 6.12-1 together with ALTAIR Hypermesh were used in preparation of the finite element model and post-processing of the results. ABAQUS Explicit V6.12-1 was used for the simulation. However, for the SPH bird, ABAQUS Explicit V6.14-1 was used.

2.1 Finite Element Model

Model and Structure Description: A typical composite sandwich wing fixed leading edge structure test specimen is shown in Figure 3. It included the J-Nose, ribs, front spar, lower panel, upper and lower covers. The front spar, ribs were made of aluminium alloys. The J-Nose sandwich panel was constructed from carbon woven fabric with a honeycomb core. The upper and lower covers were made of Carbon UD. The J-Nose is supported at the ribs and top & bottom covers and butt-strap at the lower panel.

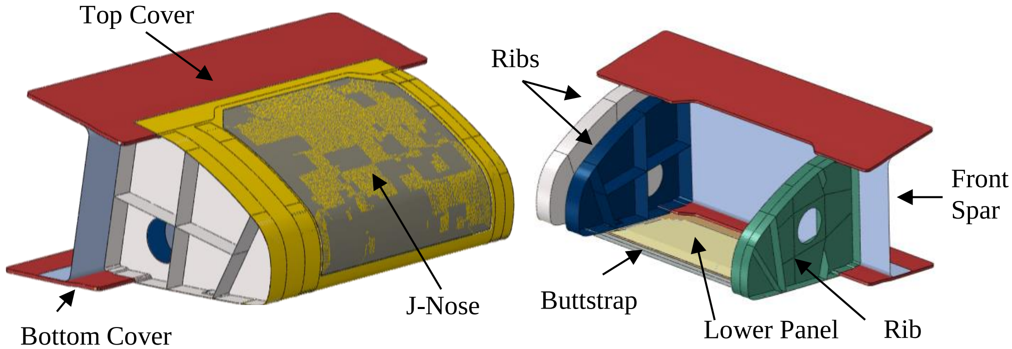

Figure 3 FE model/geometry of tested specimen

The J-Nose and Ribs were meshed using elements with edge lengths of approximately 5mm and further back the covers and spar were meshed with elements with edge lengths of approximately 10mm. The top and bottom covers were modelled as continuum shell element (SC8R) while the metallic parts ribs and front spar were modelled as shell element S4R, shown in Figure 3. The fasteners attaching various parts of the components were also included in the model using fastener modelling capabilities within ABAQUS. For the J-Nose, the skins were modelled with shell element S4R and the honeycomb was modelled using solid element C3D8R, see Figure 4. It was necessary to use triangular element and wedge element, mainly for mesh transition or corners but this was kept to a minimum. The honeycomb solid elements should be roughly cubic within practical limitations. It is assumed that the adhesive interface between skins and honeycomb is stronger than the honeycomb material which has been borne out by coupon testing. Therefore, a surface-to-surface tied interface is used to connect the skin shell elements to the solid honeycomb elements. Also, Surface-to-surface ties are used to connect the top and bottom skins together at the panel sides and at the edge of the honeycomb ramp.

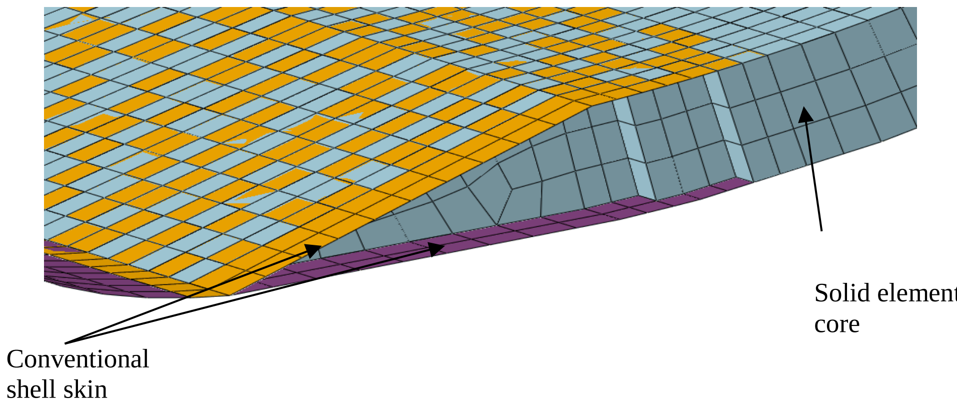

Figure 4 Modelling of the sandwich panel – J-Nose

The FE model included the full extent of the upper and lower covers, which were fully built-in in the simulation at the points where they connected to the test rig as shown in Figure 5. It was judged that these points were sufficiently far from the impact locations and the test rig is considered to be rigid.

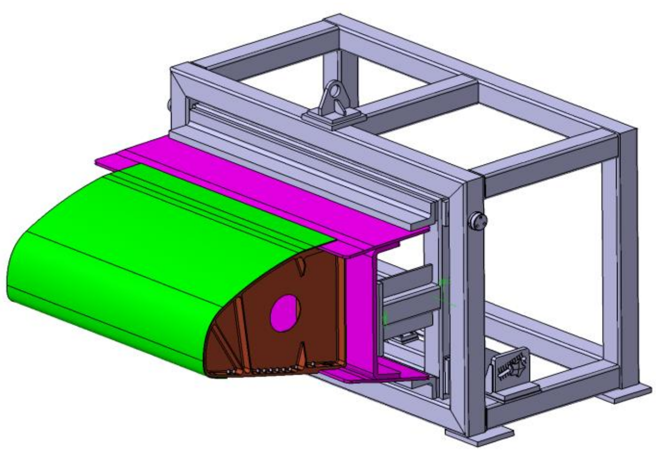

Figure 5 Specimen set up in the test rig

Material Definition: A simple orthotropic material model is used for the honeycomb which has been found to work reasonably accurately for Non-Linear Finite Element Analyses. This material model has an orthotropic elastic behaviour by defining the engineering constants and also has a plastic curve to represent the compression curve of the honeycomb. Element deletion is included. The compression true stress and true plastic strain values are input as absolute values. It is important to note that the compression curves should not include the initial peak which can occur when compressing honeycomb, shown in Figure 6, as ABAQUS cannot cope with the drop in stress for orthotropic material model. This assumption is reasonable for bird strike where cracking and/or penetration of the sandwich panel is the dominant phenomenon. However for hail or hard debris impact a more refined methodology is required and method development work is ongoing within Airbus to exploit the advanced honeycomb VUMAT capability available within ABAQUS. This would allow the peak stress in the compression curve to be retained as well as catering for non-linear shear curves. This will enable a more accurate representation of honeycomb material behaviour which may be beneficial for hard debris impacts.

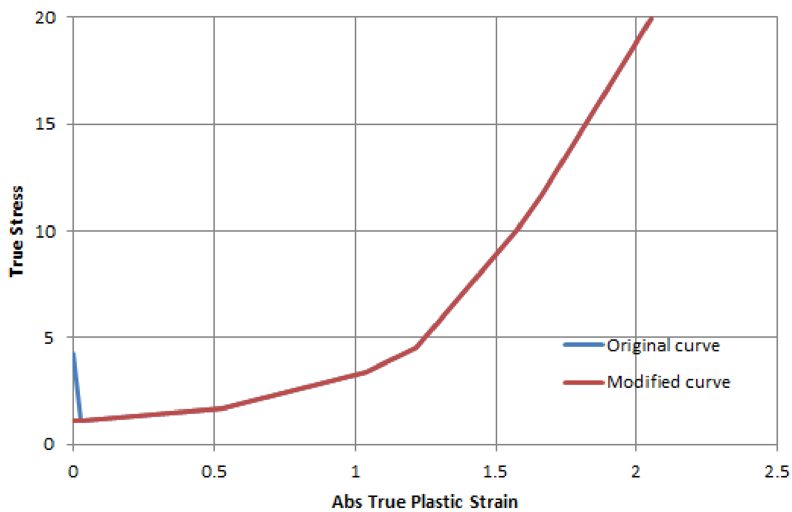

Figure 6 Compression curves with and without initial peak

The Fabric material model is used for woven (J-Nose skin) and is available as a built-in VUMAT user subroutine in Abaqus Explicit. It can be accessed by naming the material such that it begins with ABQ_PLY_FABRIC string. Non-linear in-plane shear stress-strain properties have been taken into consideration in the fabric material model. The upper and lower covers were modelled as a laminate of uni-directional plies with relevant properties in the 1 and 2 directions. True stress-strain curves up to failure for the relevant aluminium alloy were used in the analysis.

Contact Definition: General contact was defined for the whole structure so that all components can interact with each other and transfer load through the structure. A friction coefficient of 0.3 was used for the interaction between the structural components, though relative movement of these components was not anticipated.

2.2 Bird Model

Observations from high-speed film recordings have shown that the bird disintegrates upon impact and that thereafter its behaviour approximates to that of a fluid. The bird model consists of a cylinder with hemispherical ends and is shown in Figure 7 for a bird of 4 lb (1.81 kg). The length of the Bird is approximately twice its diameter. The analysis performed used a standard Lagrangian bird model developed and validated at Airbus over many years. The recommended element type is the linear hexahedral, reduced integration C3D8R element.

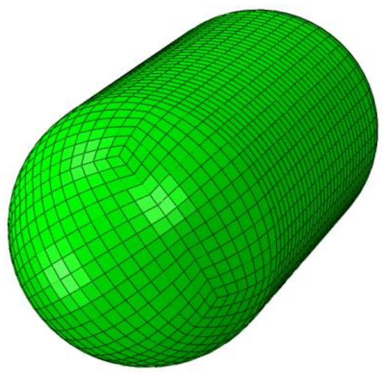

Figure 7 Bird Model

As bird flow commences on impact, the behaviour of the bird is governed by an Equation Of State which relates the pressure to the density and internal energy. It is necessary to define the failure criteria that will determine how the bird "flows". It is recommended that a small shear modulus, G, be defined, along with tensile failure, damage initiation and damage evolution, in order that elements, and therefore energy, can be removed from the bird material as it flows.

The general contact algorithm is used since it allows for a very simple definition of contact whilst using sophisticated tracking algorithms to ensure that proper contact conditions are enforced efficiently. In the analysis, it is allowed the interior of the bird to contact itself as elements erode. The contact between the bird and the structure is considered as frictionless.

2.3 Simulation Results and Correlation with Tests – Lagrangian Bird

High speed video cameras were positioned at strategic locations to provide necessary test parameters such as impact location, bird orientation on initial impact and bird dispersion which can be used in the simulation and correlation with tests. It is important to note the actual measured velocity of the bird in the test was used in the simulations. As mentioned earlier, a sample of results will be presented in this section.

2.3.1 *Damage to J-Nose but with no Bird Penetration*

The main objective of this test is to produce damage to the J-Nose without penetration. This test was performed using the configuration shown in Figure 8 with impact energy of 4.4kJ.

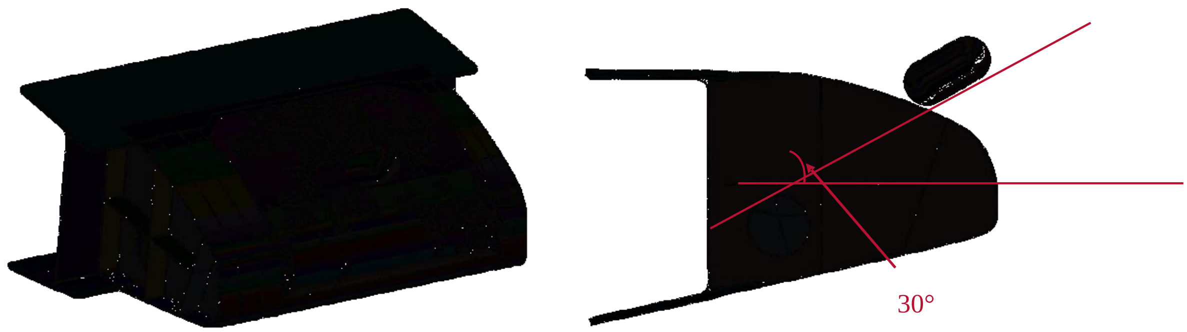

Figure 8 Bird strike set up showing the impact location on J-Nose

The NLFEA results correlated very well with the test as shown in the Figure 9. It can be seen that a through-thickness split which occurred in the test correlates well with that predicted by the analysis. The analysis captured energy level at onset of failure in panels with good accuracy. No penetration of bird debris through the panel was either predicted by the analysis or observed in the test. This impact scenario demonstrates that the analytical methods are able to capture the energy level at onset of failure in panel with good accuracy.

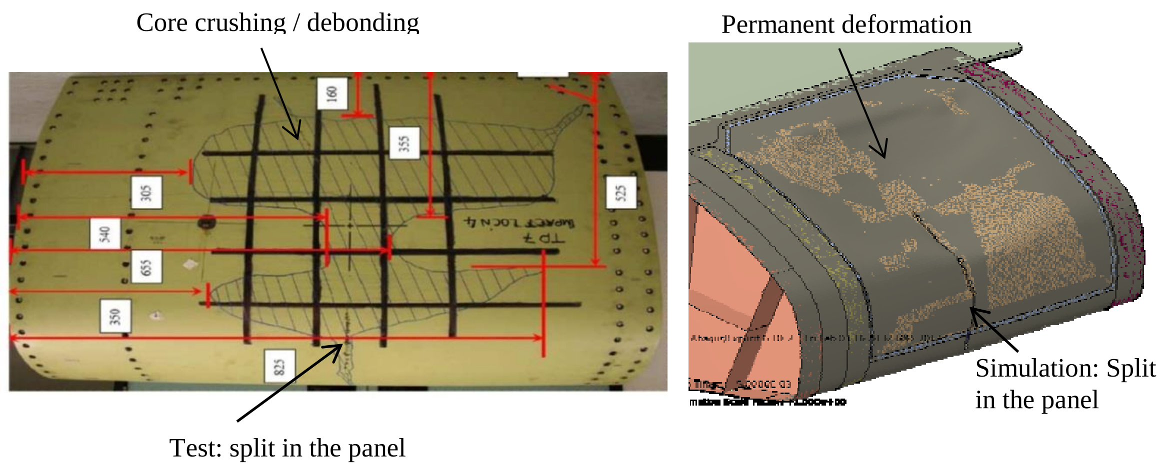

Figure 9 Damage to J-Nose but no bird penetration in both NLFEA and test

2.3.2 *Damage to J-Nose but with Bird Penetration*

The objective of this test is to produce rupture in honeycomb and monolithic laminate (i.e. bird penetration). This test was performed using the configuration shown in Figure 10 where the impact location is between the two ribs, in the middle of the J-Nose. The impact energy of this test was 12.7kJ.

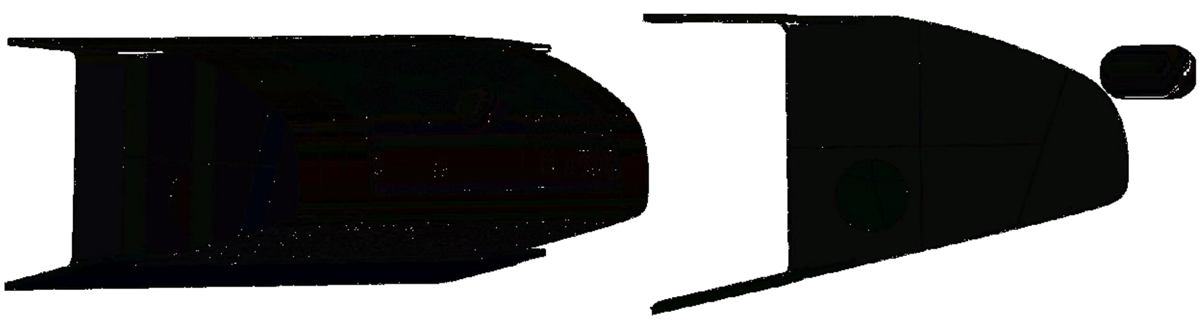

Figure 10 Bird strike set up showing the impact location on J-Nose

NLFEA predicted bird penetration of the J-Nose as observed in the test, shown in Figure 11. The simulation also predicted the level of damage severity as seen in the test.

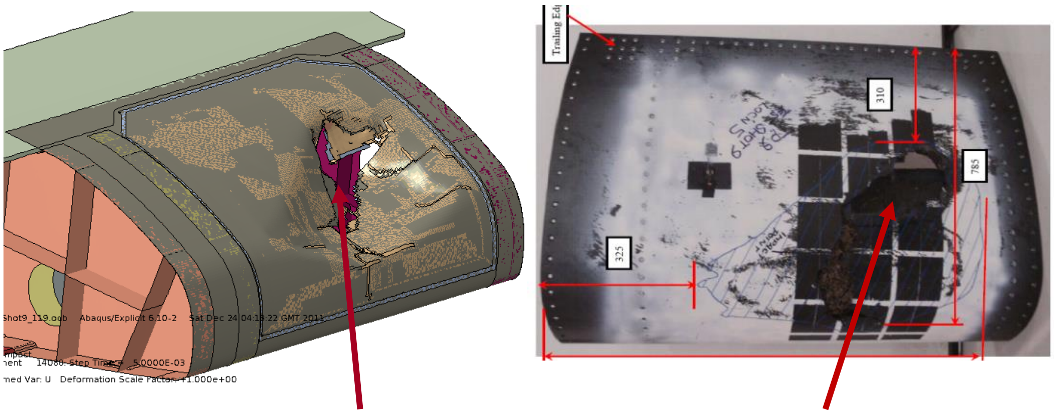

NLFEA (rupture of J-Nose) Test (rupture of J-Nose)

Figure 11 NLFEA simulation and test results correlation

2.4 Secondary Bird Impact on Witness Panel after J-Nose Penetration

In order to provide data for the developed methodology in terms of bird residual energy and dispersion of the bird after penetration, tests were performed where a metallic witness panel (2 mm thickness) was installed behind the leading J-Nose. The impact scenario was set up as shown in Figure 12. To ensure the bird impacted the witness panel after it penetrates the J-Nose, the tested specimen had a sweep angle of 15° and Angle of Attack (-6°) and bird impact energy of 8.8KJ. These parameters do not represent normal flight conditions.

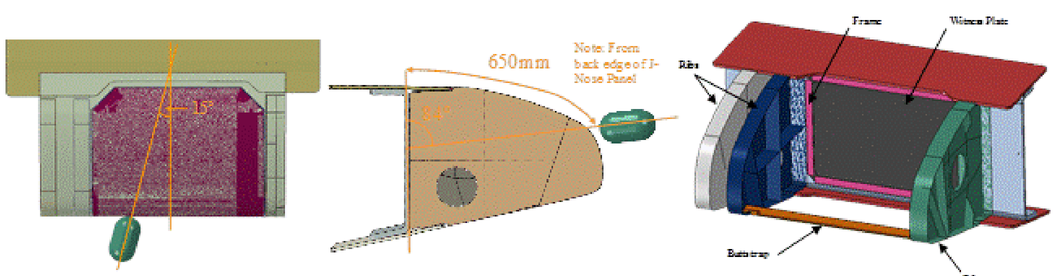

Figure 12 Impact location and witness plate installation

In both test and simulation, most of the bird penetrated the panel and showed the same level of damage of the J-Nose and bird dispersion, as shown in Figure 13 at similar time points.

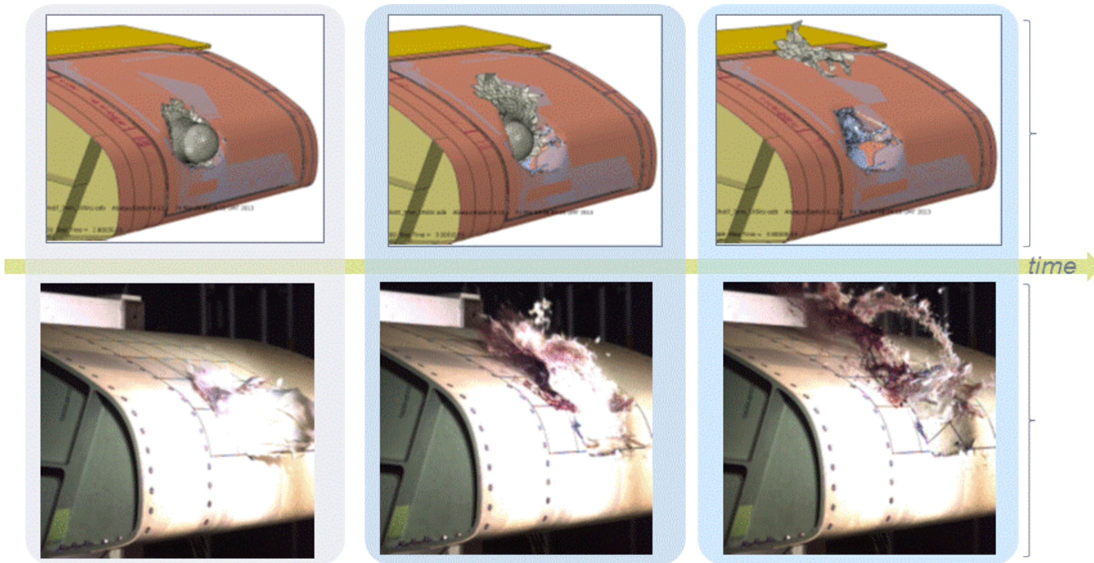

1.8 ms 3 ms 4.8 ms

Figure 13 NLFEA results (above) and test (below) results at equivalent time of impact

The energy of the bird debris impacting onto the witness plate was also accurately captured by the analysis. This is demonstrated by the close correlation of witness plate out of plane permanent deformation as shown in Figure 14. Simulation predicted maximum out of plane displacement within 0.7% of the test.

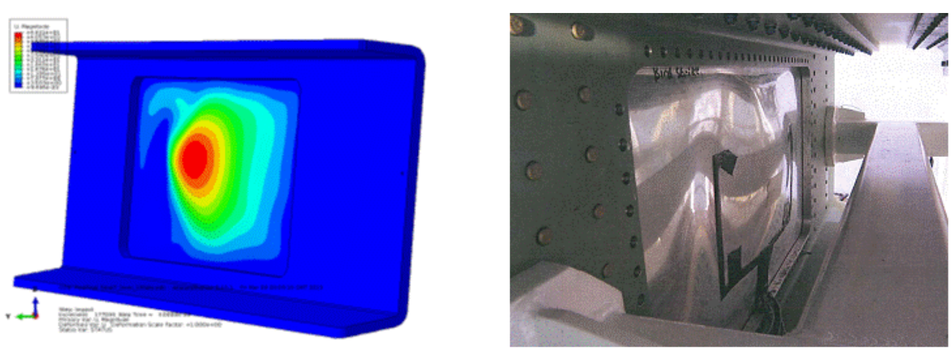

Simulation Test

Figure 14 Predicted and test permanent deformation of witness plate

The dispersion or spread of the bird debris as it penetrated the J-Nose and moved through towards the witness plate was also captured accurately by the simulation. This is demonstrated in Figure

14, which shows the bird dispersion in test and simulation at the time the bird first impacts the witness panel.

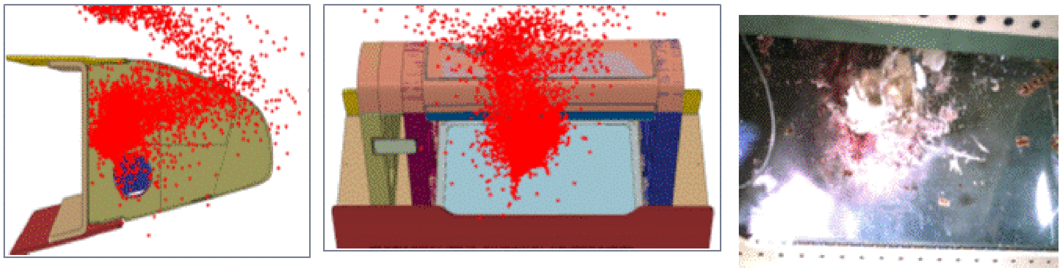

Simulation Test

Figure 14 NLFEA and test bird dispersion on impacting witness plate

The overall trend of strains measured at the rear face of the witness plate during the impact correlated well with the simulations, as shown for a typical gauge in Figure 15. This supports that the analysis captured accurately the energy and location of debris impacting the witness plate.

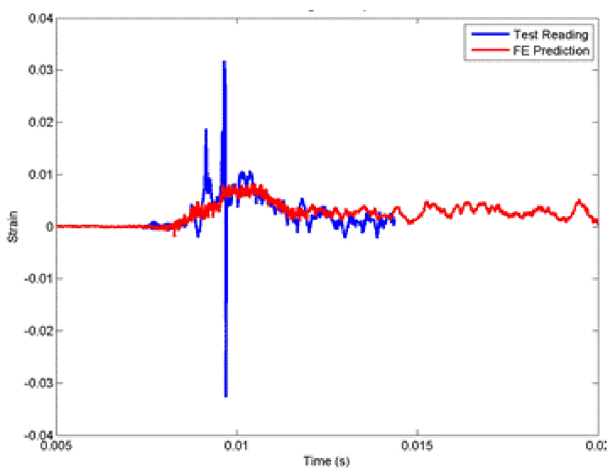

Figure 15 Strain correlations (simulation and test)

Figure 16 show the kinetic energies obtained in the simulation. The first drop in energy is caused mostly by bird impact with the J-Nose panel while the second decrease in energy is mainly due to the bird impact with the witness plate. From high-speed footage, the time interval between the bird initial impact of J-Nose and witness plate was estimated to be 8.5ms compared with 8 ms in simulation. Therefore, the average bird velocity after impact with the J-Nose was predicted well by the analysis. This coupled with the good correlation of the amount and dispersion of bird debris penetrated into the J-Nose (shown in Figures 14 and 15) indicates that the kinetic energy of the bird debris passing through the J-Nose, and therefore impacting onto the witness plate, was accurately captured.

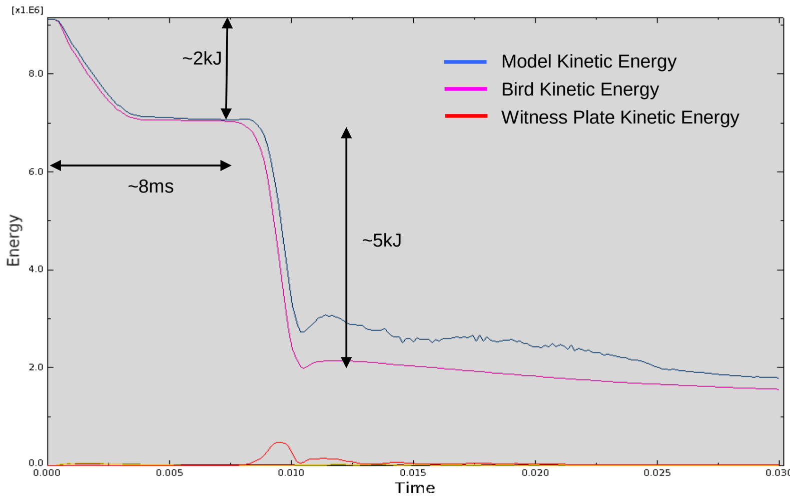

Figure 16 Model, bird and witness panel KE energy

3. Secondary Bird Impact on Witness Panel after J-Nose Penetration - SPH Bird

The new SPH capability in Abaqus/Explicit was used to perform some correlation based on the available test results. For this purpose a SPH bird model was generated with a particle arrangement of constant distances based on the Lagrangian bird geometry. Variations in particle number were carried out to identify the influence on the results. A good compromise in accuracy and run time on simple targets was found with the configuration shown in Figure 17.

Figure 17 4lb SPH bird model

The material model was not changed and taken from the Lagrangian bird model. The analysis in section 2.4 was repeated with this SPH bird model.

In the SPH bird simulation, localised rupture of the J-Nose is shown in Figure 18 and this compared well with test and simulations using Lagrangian bird (Figure 13).

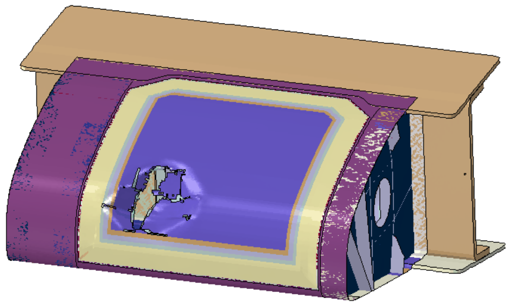

Figure 18 Rupture of the J-Nose after impact

Some bird debris deflected at the outer surface of J-Nose as shown in Figure 19, in a similar manner to Lagrangian bird simulation (Figure 13). The main bird mass travelled inside the J-Nose towards the witness plate causing it to plastically deform.

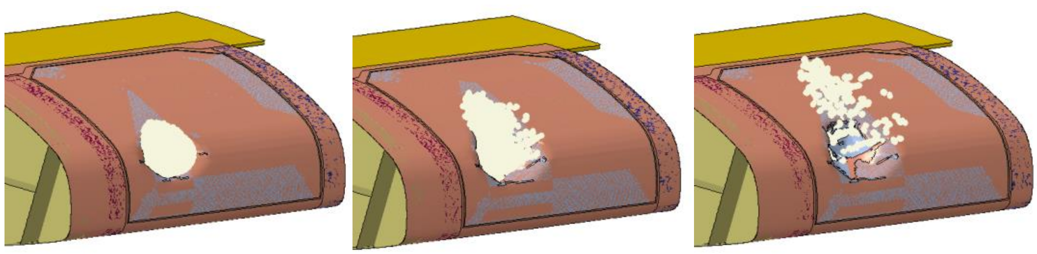

1.8 ms 3 ms 4.8 ms

Figure 18 Perforation of J-Nose using SPH bird

Localised rupture of the J-Nose is shown in Figure 19 and this compared well with test (Figure 13) and simulations using Lagrangian bird (Figure 13).

Using the SPH bird, the permanent out-of-plane displacement was predicted to be 26% less (Figure 20) compared to the test result. A potential reason identified was the deformed status of the SPH bird model just before the impact of the witness panel which showed some deviation compared to the Lagrangian bird model. For the SPH bird simulation, it was not possible to extract the energy curves as was done for Lagrangian bird (Figure 16) due to the current limitation in the code. Such correlation would have shed more light on the differences between the SPH and Lagranian results.

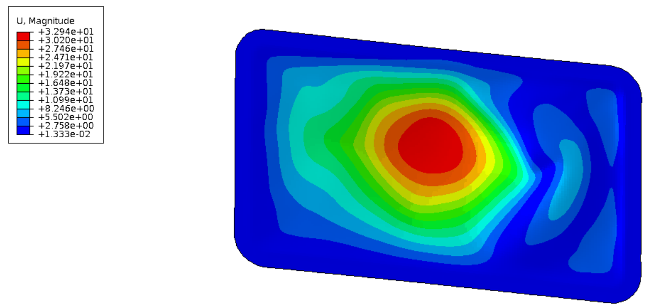

Figure 20 Deformation of witness panel in the simulation after impact

Additional test correlation activities to provide a more robust and accurate SPH bird model concerning bird strike are ongoing. Providing advantages in analysis run time and material separation the SPH approach can be a candidate to replace the Lagrangian bird model in case of more complex impact cases.

4. Conclusions

A programme of test and simulation campaign has been briefly outlined in this paper for method validation of composite sandwich structure damage prediction due to bird strike. The methodology was able not only to predict the onset of damage but also the penetration of the J-Nose and bird dispersion. The numerical methods, mainly based on Lagrangian bird, can be used with confidence for analytical work to support design on similar sandwich panel construction provided the relevant material data. Simulations were also performed using SPH bird and the results were correlated with test and Lagrangian simulation results.

5. References

[1] FAA Report, “Wildlife Strikes to Civil Aircraft in the United States 1990–2013”, National Wildlife Strike Database, July 2014.

[2] http://wildlife.faa.gov

[3] EASA Report, “Bird Strike Damage and Windshield Bird Strike”, EASA.2008.C49, 2009.

6. Acknowledgement

The authors would like to thank the contribution of David Coldbeck of Spirit AeroSystems (Europe) Ltd in providing the tests data, Richard Gibbon of Frazer-Nash for parts of the simulations and Etienne Maillard of SONACA for the valuable discussions on the simulations and providing bird impact tests on generic fixed leading structure for correlation.